Analysis of End-Loss Ion Flux for Application Studies of the Plasma Flow from the End Mirror Exit of GAMMA 10*)

Kazuya ICHIMURA, Yousuke NAKASHIMA, Katsuhiro HOSOI, Hisato TAKEDA, Takashi ISHII, Hideaki UEDA, Satoshi KIGURE, Shigehito TAKAHASHI, Satoru HOTAKA, Makoto ICHIMURA, Ryuya IKEZOE, Masayuki YOSHIKAWA, Mizuki SAKAMOTO and Tsuyoshi IMAI

Plasma Research Center, University of Tsukuba, Tsukuba, Ibaraki 305-8577, Japan

(Received 9 December 2011 / Accepted 3 August 2012)

The end-loss ion flux in GAMMA 10 is measured with a view to use it for a divertor simulation experiment or other studies that require high-performance plasma flux. First, the basic parameters of the end-loss ion flux, such as its energy and current density, were measured in typical plasma shots in GAMMA 10. A diagnostic device, the end loss ion energy analyzer (ELIEA), was used to the measure these parameters. An investigation of the relationship between the parameters of the end-loss ion flux and the plasma parameters in the central- cell revealed linear-like relationships between these parameters. We also analyzed the effects of plasma heating and fueling by using devices installed in GAMMA 10 (ion cyclotron resonance frequency (ICRF), electron cyclotron resonance heating (ECRH) and supersonic molecular beam injection (SMBI)) in order to generate more intense ion flux. The results showed that the energy distribution of the ion flux is more closely resembles a double component Maxwellian than a simple Maxwellian. Plasma heating schemes such as ECRH and ICRF are found to be effective for the generation of a more intense ion flux.

Keywords: tandem mirror, end loss, ion flux

DOI: 10.1585/pfr.7.2405147

1. Introduction

GAMMA 10 is a tandem mirror device that consists of multiple cells: the central cell, anchor cells, plug/barrier cells, and end cells (Fig. 1). The central cell is the main confinement region located at the center of GAMMA 10. The anchor cells are attached to the east and west sides of the central cell and stabilize the plasma confined in the central cell. The plug/barrier cells are located so as to form an axial confining potential in the tandem mirror system. The end cells are at the very end of GAMMA 10.

The end-loss flux of the GAMMA 10 has been focus of attention because of its applicability and extensibility for studies that require high performance plasma flux such as plasma-divertor interaction simulation experiment [1–3]. Indeed, the use of the end-loss flux for divertor simulations has already begun in GAMMA 10 and some primary results have been derived.

The features of high energy and extensibility of the GAMMA 10 end-loss flux should be noted. The core confinement plasma usually achieves a high ion temperature of several keV because of the powerful ion cyclotron resonance frequency (ICRF) devices (ICRF1 and ICRF2). Therefore, the ions in the end-loss flux are also expected to be at high temperatures. In addition, GAMMA 10 is equipped with many heat input and gas input devices (electron cyclotron resonance heating (ECRH), ICRF, neutral beam injection (NBI), gas puffing, and supersonic molecular beam injection (SMBI) equipment), and these devices increase the extensibility of the end-loss flux.

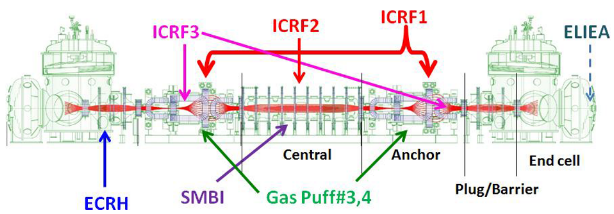

Fig. 1 GAMMA 10 vacuum vessel and positions of ICRF devices (ICRF1, 2, 3), gas puffing devices (#3, #4, #7), and ECRH and SMBI equipment.

The end-loss flux is produced in the central and anchor cells of GAMMA 10 and flows into the end cells. Therefore, experiments that require a strong plasma flux can be operated in the end cells.

2. Diagnostics

Figure 2 shows the schematic view of the GAMMA 10 west end region, together with the diagnostic tools used in this study. As a diagnostic for the end-loss ion flux, 10 units of end loss ion energy analyzer (ELIEA) are installed in each end cells in order to observe the ion flux at five

author's e-mail: ichimura_kazuya@prc.tsukuba.ac.jp

*) This article is based on the presentation at the 21st International Toki Conference (ITC21).

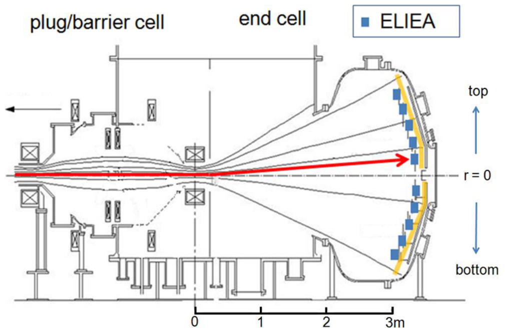

Fig. 2 ELIEA installed in the west end cell. Arrow is an example of an ion-trajectory.

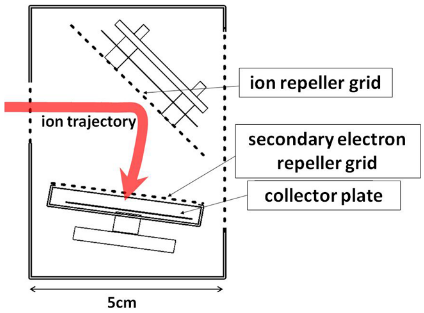

Fig. 3 Schematic diagram of ELIEA device.

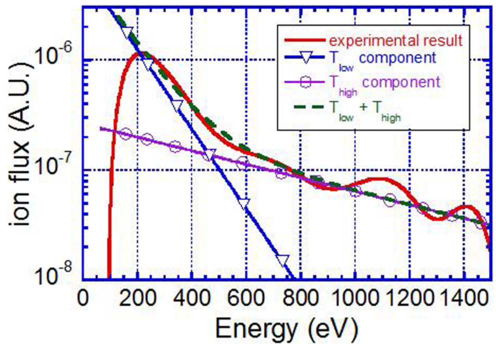

Fig. 4 Energy distribution of the ion flux measured with ELIEA and fitting curves assuming a multiple-components Maxwellian ion energy distribution.

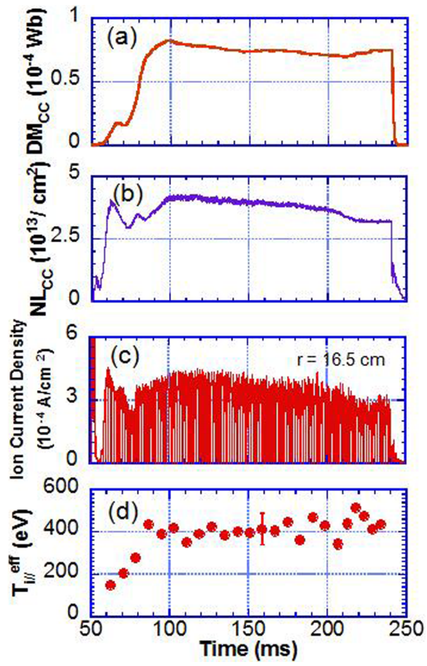

Fig. 5 Temporal evolutions of plasma parameters: (a) diamagnetism and (b) electron line density in the central-cell. (c) ion current density of ion flux. (d) parallel temperature of ion flux.

different radial positions (r = 16.5, 33.5 52.5, 71.2, and 93.2 cm) and from two different directions (top and bottom) as shown in Fig. 2.

Figure 3 shows a schematic drawing of one ELIEA device. The ELIEA is a diagnostic device consisting of three components: a slanted ion repeller grid, a secondary electron repeller grid, and a collector plate. A positive ion repeller voltage is applied to the ion repeller grid during the measurement and ions reflected by this repeller voltage are detected as an ion current by the collector plate facing the ion repeller grid as shown in Fig. 3. By sweeping the repeller voltage, the V-I characteristics of the ion flux are obtained. On the basis of these characteristics, the ion energy distribution and ion current density of the end-loss ion flux are examined [4, 5].

3. Typical Parameters of End-Loss Ion Flux

In typical GAMMA 10 operation, only the ICRF devices and gas puffing are used during a plasma shot. ICRFs (ICRF1, 2) are applied to heat the plasma, and gas puffs (GP #3, #4) are injected to supply gas.

We investigated the energy distribution of the end-loss ion flux under these experimental conditions. Figure 4 shows a typical energy distribution obtained in the present experiment. The measurements revealed that the energy distribution of the ion flux was not a simple Maxwellian distribution; a multiple-component Maxwellian, such as a combination of high-temperature and low-temperature components, well explains the actual energy distribution of the end-loss ion flux. To explain the multiple-component Maxwellian energy distribution, the effects of multiple cells in GAMMA 10 can be considered. The plasma in each GAMMA 10 cell is heated individually, and the parameters of the plasma in each cell are usually different. Therefore, the end-loss flux measured in the end cell is actually a mixture of the loss ions from each cell, producing multiple-components of the energy distribution.

Therefore, to evaluate the ion temperature of the ion flux, the effective ion temperature is calculated by averaging the value of the high-temperature and low-temperature components by taking the ratio of those components with respect to the total ion flux, as follows.

$$T_{i//}^{\text{eff}} = \beta \cdot T_{\text{high}} + (1 - \beta) \cdot T_{\text{low}}. \tag{1}$$

Figure 5 shows the time behavior of the plasma parameters and effective parallel ion temperature, $T_{i//}^{\text{eff}}$ obtained from a typical plasma shot in GAMMA 10. The characteristics of the end-loss ion flux in such a typical plasma shot are investigated, and the result (observed by the ELIEA placed at 16.5 cm above the axis) shows that the ion current density is about 0.4 mA/cm^2 and the temperature of the ion flux is about 300-400 eV parallel to the magnetic field line.

4. Parameters of Central Plasma and End-Loss-Flux

Because the end-loss ion flux is produced in the central and anchor cells of GAMMA 10, its parameters are thought to vary with the conditions of the plasma in the central and anchor cells.

To observe the relationship between the parameters of the end-loss flux and those of the confinement plasma, the former were examined under various ion-heating conditions, i.e., ICRF2 input power ranges from 40 kW to 150 kW; and gas puff (GP #3, 4) input ranges from 60 torr to 130 torr in a reservoir tank. In a GAMMA 10 plasma shot, increasing the ICRF power generally increases the diamagnetism in the central cell, DM_{CC}, which is the stored energy of the central plasma. An increase in the electron line density in the central cell NL_{CC} is generally expected when the gas puff input is increased.

Figure 6 shows the relationship between the measured parameters of the end-loss ion flux and those of the central plasma under several heating and fueling conditions. (The effects of additional heating and fueling are discussed in the next section.) The results show clear linear correlations between the ion temperature of the end-loss flux and DM_{CC}, and also between the ion-current density and NL_{CC}.

The result indicates that the energy of the end-loss ion flux rises as the energy of the central cell plasma increases, and the flux density rises as the density of the central-cell plasma is increased by gas puffing. However, upper and lower limits exist for the control of the central plasma parameters. For example, injecting too much gas causes the plasma to collapse; in addition, the ICRF power must be high enough to sustain the plasma during the discharge. Thus, to avoid plasma collapse during the operation with only ICRF and gas puffing, the ranges of DM_{CC} and NL_{CC} must be i about $0.1\text{-}0.9 \times 10^{-4}$ Wb, and $4.0\text{-}5.5 \times 10^{13}$ cm^{-2}, respectively.

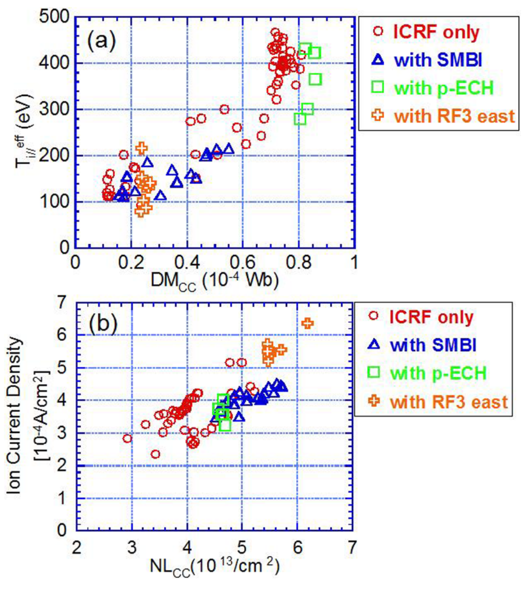

Fig. 6 Parameters of central plasma and ion flux with additional inputs applied. (a): Parallel temperature of the ion flux vs DM_{CC}. (b): Current density of the ion flux vs NL_{CC}.

5. Effects of Additional Heating Power and Gas Fueling Inputs

Suppose the end-loss flux of GAMMA 10 is applied in an experiment such as a plasma-wall interaction measurement; the energy of the ion flux is very high compared with that of conventional linear devices for plasma-wall interactions. However, the ion current density is rather small and must to be increased. Ideally, the ion flux should be increased by a factor of 10 or 100 to be relevant for the ITER SOL flux and meet the demands of various divertor simulation or plasma-wall interaction experiments [6].

To generate a more intense ion current in the end-loss flux, the use of additional inputs has been proposed. GAMMA 10 is equipped with several additional input devices. The additional inputs introduce heat or particles into the plasma in each cells of GAMMA 10; therefore the parameter range is expected to increase. Several additional inputs are tested, and some have demonstrated an ability to increase the ion current density, as shown in Fig. 6. Figure 7 shows the parameters of the central cell plasma and the ion flux during the additional inputs.

Recently, SMBI has been extensively used to improve the plasma parameters [7]. In GAMMA 10, SMBI was applied in the central cell. It inputs a large amount of gas in only a short time. The increase in the amount of gas in the central cell increases the plasma density NL_{CC}. Therefore, more ions flow into the end cells, and the ion-current density is increased during SMBI. In the present experiment, SMBI allowed as to obtain parameters that could not be achieved in typical discharge conditions: NL_{CC} value of 5.8×10^{13} cm^{-2} and an ion current density of 0.45 mA/cm^2. However, gas injection causes a loss in ion energy in the central cell (DM_{CC}), which decreases the energy of the end-loss flux. The value of the end-loss ion temperature in such sequence is evaluated as about 100-200 eV, which is much lower than a typical ion temperature (around 400 eV). In addition, if too much gas is injected,

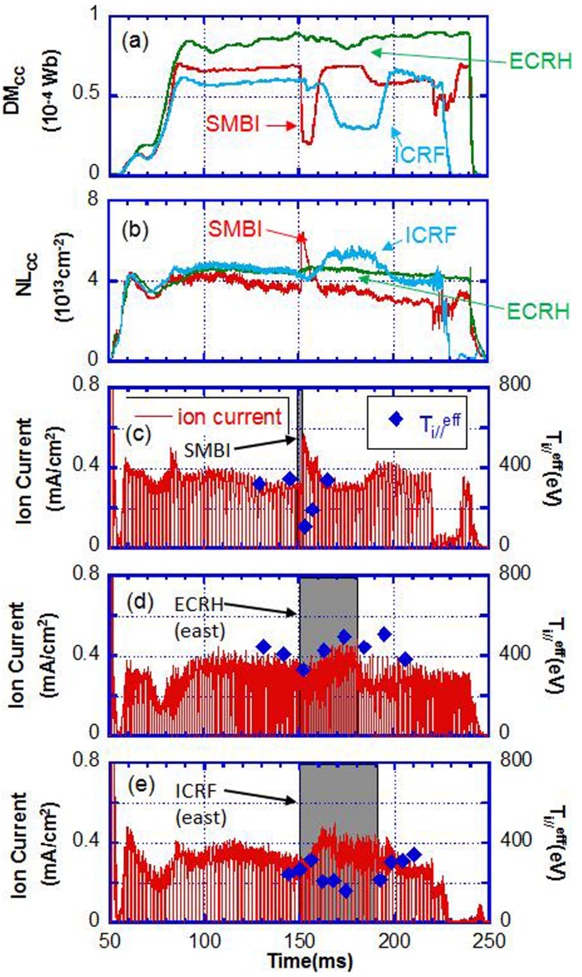

Fig. 7 Temporal behaviors of plasma parameters in SMBI, ECRH, and ICRF3 experiments. (a) Diamagnetisms of central cell. (b) Electron line density of central cell. Ion current density and ion temperature of end-loss ion flux in (c) SMBI, (d) ECRH and (e) ICRF3.

the plasma will collapse.

ECRH is applied to the east plug/barrier cell in order to form a positive confining potential. With the confining potential, ions flowing to the east end cell are reflected by the potential, and the amount of ion flow increases in the west end-cell. The ion current density with the potential is about 20-30% higher than that without the potential. Note that the large loss in the ion energy that occurred in gas injection was not observed in ECRH input. If the confining potential reflected the ion flux toward the east very effectively, the ion flux in the west end would be expected to double. However, inadequate confinement potential formation may enhance the radial loss in ions; consequently, ion flux in the west end increased by only 20-30 % in the experiment.

An ICRF pulse (ICRF3) was superimposed on the east and west anchor cells individually. In both cases, an increase in the ion current density was observed. During superimposition of ICRF3 into the east anchor cell, the ion current density and NL_{CC} increased, as shown in Fig. 7 (e). With the superimposing of ICRF3, more plasma is produced in the anchor cell, and the increased density in there makes the entire plasma more magnetohydrodynamically stable. As a result, the maximum value of the controllable NL_{CC} range increased, as shown in Fig. 6. Because the higher NL_{CC} is achieved by ICRF3 input, a higher ion flux is achieved compared with that in experiments without ICRF3. This result indicates that the additional ICRF heating is effective for increasing the ion flux.

6. Summary

The end-loss-ion-flux of GAMMA 10 was analyzed by using the ELIEA. Typical parameters are anion current density of 0.4 mA/cm^2 and an ion temperature of 400 eV. The results will contribute to future divertor simulations or other studies in GAMMA 10.

To generate a more intense ion flux, the effects of several additional inputs were examined. Gas injection increases the ion current density and decreases the ion energy. The formation of a confining potential by ECRH input also increases the ion current density. Superimposition of ICRF (ICRF3) in the east anchor cell greatly increased the ion flux. These results suggest that GAMMA 10 can generate a more energetic, denser ion flux with the help of additional inputs such as ICRF heating and ECRH. The maximum ion current density achieved to date is 0.65 mA/cm^2; the optimization and installation of additional inputs in order to obtain more high-performance ion flux will be discussed in future.

Acknowledgement

This study was supported by the NIFS as bidirectional collaborative research (NIFS09KUGM037). The author thanks the members of the GAMMA 10 research group for their collaboration on the experiments and for helpful discussions.

[1] Y. Nakashima *et al.*, Fusion Eng. Des. **85**, 956 (2010).
[2] Y. Nakashima *et al.*, Trans. Fusion. Sci. Technol. **59**, 61 (2011).
[3] Y. Nakashima *et al.*, J. Nucl. Mater. **415**, s996 (2011).
[4] T. Kuwabara *et al.*, Rev. Sci. Instrum. **65**, 936 (1994).
[5] A.W. Molvik, Rev. Sci. Instrum. **52**, 704 (1981).
[6] K. Shimizu *et al.*, J. Plasma Fusion Res. **80**, 183 (2004).
[7] T. Mizuuchi *et al.*, Contrib. Plasma Phys. **50**, No.6-7, 639 (2010).